Published in final edited form as:
J Control Release. 2013 December 28; 172(3): . doi:10.1016/j.jconrel.2013.09.010.

Differential immunotoxicities of poly(ethylene glycol)-*vs*. poly(carboxybetaine)-coated nanoparticles

Mahmoud Elsabahy[1,2,*], **Ang Li**[1], **Fuwu Zhang**[1], **Deborah Sultan**[3], **Yongjian Liu**[3], and **Karen L. Wooley**[1,*]

[1]Department of Chemistry, Department of Chemical Engineering, Laboratory for Synthetic-Biologic Interactions, Texas A&M University, P.O. Box 30012, 3255 TAMU, College Station, Texas 77842-3012, USA

[2]Department of Pharmaceutics, Faculty of Pharmacy, Assiut Clinical Center of Nanomedicine, Al-Rajhy Liver Hospital, Assiut University, Assiut, Egypt

[3]Department of Radiology, Washington University in Saint Louis, MO 63110, USA

Abstract

Although the careful selection of shell-forming polymers for the construction of nanoparticles is an obvious parameter to consider for shielding of core materials and their payloads, providing for prolonged circulation *in vivo* by limiting uptake by the immune organs, and thus, allowing accumulation at the target sites, the immunotoxicities that such shielding layers elicit is often overlooked. For instance, we have previously performed rigorous *in vitro* and *in vivo* comparisons between two sets of nanoparticles coated with either non-ionic poly(ethylene glycol) (PEG) or zwitterionic poly(carboxybetaine) (PCB), but only now report the immunotoxicity and anti-biofouling properties of both polymers, as homopolymers or nanoparticle-decorating shell, in comparison to the uncoated nanoparticles, and Cremophor-EL, a well-known low molecular weight surfactant used for formulation of several drugs. It was found that both PEG and PCB polymers could induce the expression of cytokines *in vitro* and *in vivo*, with PCB being more immunotoxic than PEG, which corroborates the *in vivo* pharmacokineties and biodistribution profiles of the two sets of nanoparticles. This is the first study to report on the ability of PEG, the most commonly utilized polymer to coat nanomaterials, and PCB, an emerging zwitterionic anti-biofouling polymer, to induce the secretion of cytokines and be of potential immunotoxicity. Furthermore, we report here on the possible use of immunotoxicity assays to partially predict *in vivo* pharmacokineties and biodistribution of nanomaterials.

Keywords

Poly(ethylene glycol); poly(carboxybetaine); Cremophor-EL; protein adsorption; stealth; antibiofouling; immunotoxicity; cytokines; nanoparticles; pharmacokineties; biodistribution

The use of multifunctional nanomaterials for various biomedical applications is currently receiving great impetus, but there are important side effects of such materials that are being

*Correspondence to: mahmoud.elsabahy@chem.tamu.edu, wooley@chem.tamu.edu (Tel.: +1 979 845 4077; Fax: +1 979 862 1137).

neglected [1–4]. Design of safe yet efficient nanocarriers depends on understanding the mechanisms *via* which they are formed, and on testing toxicity, stability and intracellular fate of nanoparticles and their constituents. In addition to studying the effect of size, morphology and surface charge on the *in vitro* and *in vivo* characteristics of nanoparticles, selection of an appropriate polymer to form a shell around the nanoparticle core is a high priority, as it dictates the initial interactions between nanoparticles and the surrounding environments (*i.e.* other nanoparticles, blood, plasma proteins, extracellular- and intracellular-biomolecules). Poly(ethylene glycol) (PEG) is the most commonly utilized polymer to impart steric stability to nanoparticles, as well as to prolong the blood-circulation time and to reduce the immunogenicity of nanomaterials. However, there has been continued interest in finding alternative hydrophilic polymers that can impart better "stealth" properties, biocompatibility and sustained *in vivo* circulation. Examples of these polymers include poly(acrylic acid) (PAA), poly(*N*-vinylpyrrolidone), poly(*N*-isopropylacrylamide) and poly(carboxybetaine) (PCB) [5–10]. In particular, zwitterionic PCB was developed to impart high anti-biofouling properties to the coated nanoparticles, possibly due to electrostatically binding water molecules more tightly than the hydrogen bonding displayed in other hydrophilic polymers (*e.g.* PEG) and, thus, resulting in higher hydration of the corona [8–10]. Effective hydration is critical in minimizing the protein adsorption and in imparting stealth properties to nanoparticles. It has been reported recently that the use of PCB instead of PEG enhances the bioactivity of the conjugated proteins, whereas both polymers had a similar stabilizing effect on the conjugated proteins [10]. Although pharmacokinetics and biodistribution studies are becoming increasingly common, still the molecular-level effects of nanomaterials are investigated to a lesser extent and the roles of nanomaterials in generating immunotoxic effects requires significantly greater attention.

Nanoparticles can interact with various components of the immune system and either enhance or inhibit its function, where induction of proinflammatory cytokines can be a useful tool for the partial prediction of nanoparticle immunotoxicity [1, 11–14]. For instance, systemic administration of cationic protamine DNA lipoplexes to mice resulted in production of large amounts of proinflammatory cytokines (TNF-α, IL1-β, IL-12 and IFN-γ), which were associated with toxicities in animals [15]. In a recent study, we have demonstrated that partial modification (15%) of cationic nanoparticles with histamine (instead of primary amines) significantly reduced the toxicity and immunotoxicity of the nanoparticles as indicated by the lower secretion of cytokines *in vitro* upon treatment of RAW 264.7 mouse macrophages with the nanoparticles, probably due to the lower charge density (*i.e.* lower primary amine content) [16].

Often, the *in vitro* behaviors of synthetic materials determined in simple assays do not correlate with their *in vivo* responses. PEG, PCB and other hydrophilic polymers usually do not show significant cellular toxicity *in vitro*, resulting in similar cell viability to the controlled untreated cells over the range of tested concentrations. *In vivo*, it is always difficult to conclude which components of nanoparticles are responsible for any resulting toxicity, or whether it is rather an additive effect. Utilizing homopolymer controls, either *in vitro* or *in vivo*, is not necessarily valuable because these polymers behave differently in unimers and aggregated forms. We have previously synthesized poly(acrylic acid)-*block*-polylactide (PAA-*b*-PLA) copolymers and utilized the PAA shell to graft PEG and PCB of various molecular weights, and to further study the effects of these structural modifications on the physicochemical characteristics and *in vivo* pharmacokinetics and biodistribution of the nanoparticles [17]. Significant differences in the physicochemical properties and *in vivo* characteristics were found between the shell crosslinked knedel-like nanoparticles (SCKs) grafted with PEG and PCB of varying molecular weights. The available data to explain differences between the two sets of polymeric coatings were the physicochemical characteristics of SCKs- size and zeta-potential- although several questions were left open.

The goal of the current work is to compare cytotoxicity, immunotoxicity, and anti-biofouling competencies of PEG and PCB as potential shell-forming polymers for a wide range of therapeutic and diagnostic nanoparticles, aiming to provide additional explanations for the differences in pharmacokinetics of nanoparticles. The effect of polymers, either as homopolymers or shell-forming polymers of nanoparticles, on immunotoxicity and protein-adsorption capabilities of the nanoparticles was studied. In addition, uncoated nanoparticles and Cremophor-EL, were utilized as controls to further understand the effect of nanoparticle composition and structure on biological interactions between nanoparticles and cells, and to evaluate the potential of utilizing these nanoparticles as alternatives to one of the vehicles that is commonly employed for formulation of drugs, respectively. It was found that both PEG and PCB polymers can be immunotoxic, although PCB-based nanoparticles induced a higher release of proinflammatory cytokines, both *in vitro* and *in vivo*, than did PEG-SCKs. The data presented here highlight the possible immunotoxicity of polymers that are well-known for their biocompatibility and open the venue for further investigation and characterizations. In addition, they provide a new measure that can partially contribute to predicting the *in vivo* pharmacokinetics and clearance of a particular nanoparticle formulation.

METHODS

Synthesis of block copolymers and preparation of the SCKs

The preparation of the degradable SCKs was reported previously [17]. The amphiphilic diblock copolymer poly(acrylic acid)$_{75}$-*b*-poly(lactide)$_{33}$ (PAA$_{75}$-*b*-PLA$_{33}$) was synthesized by sequential reversible addition-fragmentation chain transfer (RAFT) polymerization of *tert*-butyl acrylate (*t*BA) with AIBN as the thermal radical initiator and ring opening polymerization of lactide using 1,8-diazabicyclo[5.4.0]undec-7-ene (DBU) as the organo-catalyst, followed by the treatment of trifluoroacetic acid (TFA) to remove the *tert*-butyl groups. The multifunctional grafted polymer precursors were afforded by an amidation reaction between carboxylic acid groups from PAA$_{75}$-*b*-PLA$_{33}$ and primary amine groups of PEG or PCB polymers, 2-aminoethyl-mono-amide-DOTA-tris (*t*Bu ester) and tyramine. The DOTA and tyramine were incorporated for the purpose of potential radiolabeling. The SCKs were then constructed by direct dissolving grafted polymers into nanopure water to form micelles, followed by crosslinking with 2,2'-(ethylenedioxy) bis(ethylamine) (EDDA) with 20% nominal crosslinking.

Dynamic light scattering and zeta-potential measurements

The nanoparticles were characterized in terms of size, polydispersity index and zeta-potential using Delsa Nano C (Beckman Coulter, Inc., Fullerton, CA) equipped with a laser diode operating at 658 nm. Scattered light was detected at a 165° angle and calculation of the particle size distribution and distribution averages was performed using CONTIN particle size distribution analysis routines.

Cytotoxicity assay

The cytotoxicity assay has been carried out as reported previously [16]. RAW 264.7 (2×10^4 cells/well) mouse macrophages were plated in 96-well plate in Dulbecco's Modified Eagle Medium (DMEM) (10% fetal bovine serum and 1% penicillin/streptomycin). Cells were incubated at 37 °C in a humidified atmosphere containing 5% CO_2 for 24 h to adhere. Then, the medium was replaced with a fresh medium 1 h prior to the addition of 20 μL of the PEG and PCB homopolymers, PEG- and PCB-SCKs to 100 μL of the medium (final concentrations ranged from 5–500 μg/mL). The cells were incubated with the formulations for 24 h and washed once with phosphate-buffered saline (PBS) and 100 μL of the complete media was added to the cells. MTS combined reagent (20 μL) was added to each well (Cell

Titer 96® Aqueous Non-Radioactive Cell Proliferation Assay, Promega Co., Madison, WI). The cells were incubated with the reagent for 2 h at 37 °C in a humidified atmosphere containing 5% CO_2 protected from light. Absorbance was measured at 490 nm using SpectraMax M5 (Molecular Devices Co., Sunnyvale, CA). Cell viability was calculated based on the relative absorbance to the control-untreated cells. The calculation of the IC_{50} values and the statistical analysis were performed using GraphPad Prism four-parameter fit, considering the 0% and 100% cell viabilities are for the control medium (no cells) and cells with no treatment, respectively.

Multiplex assay

The multiplex assay has been performed as reported previously [16]. The RAW 264.7 cells were treated with medium (control), Cremophor-EL, PEG and PCB homopolymers, PEG- and PCB-SCKs (500 μg/mL) for 24 h. The SCKs prepared without grafting PEG and PCB polymers (*i.e.* PAA_{75}-*b*-PLA_{33} SCKs), functionalized or not with DOTA and tyramine, were utilized also as controls at the same concentration of 500 μg/mL under the same experimental conditions. The supernatants were then collected and centrifuged for 10 min at 13,000 rpm. Serial dilutions of cytokine standards were also prepared in the same diluent utilized for the samples (*i.e.* cell-culture medium). Control, standards and nanoparticle-treated samples (50 μL) were incubated with antibody-conjugated magnetic beads for 30 min in the dark. After washing, the detection antibody was added to the wells and incubated in the dark for 30 min under continuous shaking (300 rpm). After washing, streptavidin-phycoerythrin was added to each well and incubated while protected from light for 10 min under the same shaking conditions. Finally, after several washings and re-suspension in the assay buffer and shaking, the expression of the mouse cytokines, interleukin (IL)-1α, IL-1β, IL-2, IL-3, IL-4, IL-5, IL-6, IL-9, IL-10, IL-12 (P40), IL-12 (P70), IL-13, IL-17, Eotaxin, granulocyte-colony-stimulating factor (G-CSF), granulocyte macrophage-colony-stimulating factor (GM-CSF), interferon-γ (IFN-γ), keratinocyte-derived chemokine (KC), monocyte chemotactic protein (MCP)-1, macrophage inflammatory protein (MIP)-1α, MIP-1β, regulated upon activation normal T-cell expressed and presumably secreted (RANTES) and tumor necrosis factor-α (TNF-α) was measured immediately using Bioplex 200 system with HTF and Pro II Wash station and the data was analyzed using the Bioplex Data Pro software (Bio-Rad Laboratories, Inc., Hercules, CA).

Protein adsorption assay

Adsorption of the mouse cytokines, IL-1α, IL-1β, IL-2, IL-3, IL-4, IL-5, IL-6, IL-9, IL-10, IL-12 (P40), IL-12 (P70), IL-13, IL-17, Eotaxin, G-CSF, GM-CSF, IFN-γ, KC, MCP-1, MIP-1α, MIP-1β, RANTES and TNF-α by Cremophor-EL, PCB polymer, PEG polymer, PCB-SCKs and PEG-SCKs, was measured using a Bioplex 200 system with HTF and Pro II Wash station. Specific concentrations of the standards of each cytokine were determined either in cell culture medium (the same medium used in the multiplex assay section) or when mixed with the various polymers and nanoparticles (500 μg/mL polymers or nanoparticles) in the same medium, as has been described in the previous section. The values are presented as the ratio of the cytokines in the cytokines/nanoparticles mixture to the solution that contain the same amount of the cytokines but without the nanoparticles.

In vivo immunotoxicity assay

Male C57 mice (8 weeks, Charles River Laboratories, Wilmington, MA) were administered 4 mg/kg (*ca.* 100μL) of Cremophor-EL, PEG_{5k}-SCKs and PCB_{5k}-SCKs that were prepared in PBS *via* tail vein injection (n=3). The mice were sacrificed 3 h post injection and blood was drawn into a BD Microtainer Serum Separator Tube (BD, Franklin Lakes, NJ), allowed to clot by leaving it undisturbed for 30 min and centrifuged for 5 minutes at 13,460 *g* using a

Thermo IEC Micro-MB centrifuge. The supernatants were then collected, frozen and kept for further analysis of concentrations of cytokines. The serum samples were further centrifuged for 10 min at 13,000 rpm 4 °C prior to analysis. Then, 50 μL of serum was diluted with 150 μL with the Bioplex sample diluent. Serial dilutions of cytokine standards were also prepared in the same Bioplex sample diluent utilized for the serum samples. Control serum, standards and serum samples of animals treated with Cremophor-EL and nanoparticles (50 μL) were incubated with antibody-conjugated magnetic beads for 30 min in the dark and quantified as mentioned in the multiplex assay section.

Endotoxin assay

The endotoxin contents of the various samples were measured by using the Pierce® Limulus Amebocyte Lysate (LAL) Chromogenic Endotoxin Quantitation Kit, according to the manufacturer instructions. Briefly, all reagents were equilibrated to the room temperature, while the 96-well microplate was maintained at 37 °C. To each well, 50 μL of each endotoxin standards, blank (endotoxin-free water), Cremophor-EL, polymers and SCKs was dispensed and the plate was covered and incubated for 5 min at 37 °C. Then, 50 μL of LAL was added to each well, gently agitated for 10 seconds and incubated again for 10 min at 37 °C, followed by the addition of 100 μL of substrate solution. After gentle agitation and incubation for 6 min at 37 °C, 50 μL of 25% acetic acid (stop reagent) was added to each well and the absorbance was measured at 405 nm using SpectraMax M5. The concentration of endotoxin in the standards and samples was determined after constructing a standard curve from the corrected absorbance values.

Statistical analysis

Values are presented as mean ± SD of at least three independent experiments. Significance of the differences between two groups was evaluated by Student's t test (unpaired) or between more than two groups by one-way ANOVA followed by Tukey's multiple comparison tests. Differences between different groups were considered significant for p values less than 0.05.

RESULTS AND DISCUSSION

Preparation and characterization of PEG-*g*-PAA-*b*-PLA SCKs and PCB-*g*-PAA-*b*-PLA SCKs

We have previously developed facile and effective methods for the preparation of well-defined multifunctional nanomaterials with tunable characteristics [3, 4, 16–18]. SCKs are constructed *via* self-assembly of amphiphilic copolymers into polymeric micelles, followed by crosslinking some of the functionalities in the shell layer to form robust nanostructures, with possibility of further functionalizing the surface of the nanoparticles with various polymeric coatings, targeting moieties, imaging probes, and/or other agents [3, 19]. SCKs have been developed to overcome potential dissociation upon *in vivo* dilution of polymeric micelles to a concentration below the critical micelle concentration. In addition, we and others have recently shown that crosslinking enhances the kinetic stability of nanoparticles, preserves their structures during the lyophilization process, provides greater protection for the encapsulated cargoes, prolongs their circulation time and allows high accumulation at the target diseased-areas [3, 4, 20–22] Crosslinking also has other applications in other materials designs, for example, in the preparation of gels and nanocages and in stabilizing drug crystals [3, 23–25].

PAA-*b*-PLA has recently been synthesized and reversible addition-fragmentation chain transfer (RAFT) polymerization was utilized to synthesize PCB grafts of comparable molecular weights to PEG grafts to investigate the *in vivo* pharmacokinetics of PEG- *vs.* PCB-based SCKs [17]. DOTA (1,4,7,10-tetraazacyclododecane-1,4,7,10-tetraacetic acid)

chelator and tyramine were also covalently incorporated for positron emission tomography imaging and potential therapy. In this study, amphiphilic block graft copolymers having 2 and 5 kDa PEG or PCB polymers grafted onto PAA-*b*-PLA chains (5 grafts *per* PAA chain) were synthesized and functionalized with DOTA and tyramine, followed by self-assembly in water to yield micelles that were further crosslinked to form the multifunctional SCKs (Figure 1A). The sizes and zeta-potentials of the formed particles were measured at pH 7.4 (Tris buffer, 10 mM) (Table 1). Each nanoparticle had a number-averaged hydrodynamic diameter that ranged from 18–31 nm, except for the PCB_{2k}-SCKs which exhibited a diameter of *ca.* 90 nm (Figure 1B and Table 1). The 5 kDa polymeric chains (both PEG and PCB) shielded the negative charge of PAA and resulted in almost neutral nanoparticles that had zeta-potential values of −0.3 and −4.5 mV, respectively (Table 1). In contrast, the 2 kDa grafted PEG and PCB polymers resulted in nanoparticles with overall negative zeta-potential values (− 27 and − 36 mV, respectively). This study was focused mainly on the SCKs grafted with 5 kDa PEG and PCB polymers because they provided better shielding for the nanoparticles, as indicated by the almost neutral zeta-potential values, and due to their better *in vivo* pharmacokinetics and biodistribution profiles demonstrated in the previous study [17]. In addition, as control experiments, the uncoated nanoparticles, functionalized or not with DOTA and tyramine, were prepared and their sizes and zeta-potentials were measured (Table 1). SCKs that were not functionalized with PEG or PCB had larger sizes, broader size distributions and higher negative zeta-potential values (in particular, as compared to the PEG_{5k}- and PCB_{5k}-SCKs), which highlights the benefits from the steric stability imparted by the PEG and PCB polymers of higher molecular weights. Both PEG_{5k}- and PCB_{5k}-SCKs had similar size distribution and zeta-potential values (Figure 1B and Table 1), although the number-, volume- and intensity-averaged hydrodynamic diameters of the PCB-based SCKs were slightly larger. In the previous study, the measurements of size and zeta-potentials were carried out in nanopure water (pH *ca.* 5.5) [17]. At pH 7.4, the physicochemical properties were significantly different, which might be due to the presence of charged polymeric species (*e.g.* PAA and PCB) that can have different ionization degrees and conformations at different pHs.

In vitro cytotoxicities and immunotoxicities of PEG- and PCB-SCKs *versus* Cremophor-EL

The goal of performing the cytotoxicity assay of PEG and PCB-based nanoparticles was to confirm that the immunotoxicity assays would be performed at non-cytotoxic concentrations. At the concentration range of 5–500 μg/mL, both types of SCKs were non-toxic to RAW 264.7 mouse macrophages after 24 h of incubation and there were no significant differences between them (data not shown). Except for cationic materials, the low cytotoxicity of unloaded nanoparticles at this concentration range is consistent with other studies. For instance, we have not observed any cytotoxicity in RAW 264.7 mouse macrophages after treatment with nonionic, anionic and zwitterionic polyphosphoester-based micelles at a concentration range of 5–1000 μg/mL after incubation with cells for 24 h, although similar cationic micelles showed dose-dependent cytotoxicity [26].

One of the valuable tools in screening nanoparticle immunotoxicity and in studying the relationship between nanoparticle composition and the resulting toxicity is the measurement of enhancement in secretions of cytokines, in particular proinflammatory cytokines, following the incubation of cells with the nanoparticles or after *in vivo* administration [1]. It is a prerequisite that biocompatible nanoparticles should not induce a massive release of cytokines, unless it is desirable. We previously have shown that incorporation of histamine into the shell composition of cationic SCKs reduced the release of cytokines in mouse macrophages, as compared to the unmodified (shell formed entirely of primary amines) nanoparticles [16]. In the current study, PEG- and PCB-coated nanoparticles were incubated with the RAW 264.7 mouse macrophages at a non-cytotoxic concentration (500 μg/mL) for

24 h, followed by measurement of the levels of 23 cytokines utilizing a multiplex assay, as described previously [16]. PCB_{5k}-SCKs significantly induced the production of several cytokines, as compared to PEG_{5k}-SCKs and the control-untreated cells (Figure 2). The PEG_{5k}-SCK was significantly different from the control for only one cytokine MCP-1 (p = 0.012), and significantly resulted in higher release than the PCB-coated nanoparticles for the same cytokine (p = 0.03). PCB_{5k}-SCK was significantly different from the control for twenty cytokines with low p values, and resulted in higher induction of 17 cytokines, as compared to PEG-SCKs. In particular, higher secretions of IL-1β, IL-4, IL-12 (p70), KC, MCP-1 and MIP-1α were observed in cells treated with the PCB_{5k}-SCKs, as compared to PEG_{5k}-SCKs (p values < 0.05 and 0.001 for MIP-1α) (Figure 2). Cremophor-EL, a well-known low molecular weight surfactant for inducing hypersensitivity reactions and peripheral neuropathy *in vivo* [27], induced lower immunotoxicity than these nanoparticles (Figure 2). As compared to the control, Cremophor-EL (500 μg/mL) induced higher expression of IL-3 (p = 0.03), MIP-1α (p = 0.002), and MIP-1β (p = 0.005). Dose-dependent induction for MIP-1α was observed for the Cremophor-EL when concentration increased from 50 to 500 μg/mL (p = 0.007, data not shown). The *in vivo* reported toxicity associated with the administration of Cremophor-EL may result from other factors, which can be involved in the cascade that leads to the hypersensitivity reactions.

The PCB and PEG homopolymers (5 kDa) were used as controls to test their cytotoxicity, immunotoxicity and anti-biofouling properties, in comparison to PEG_{5k}- and PCB_{5k}-based SCKs and Cremophor-EL surfactant. As for the nanoparticle materials, the PCB and PEG homopolymers exhibited no cytotoxic effects when measured at up to 500 μg/mL concentrations. However, the unique cellular response differences were revealed by the immunotoxicity assays of the free polymers *vs*. their nanoparticle analogs. No cytokine secretions were induced by the free polymers (PEG or PCB) at various tested concentrations (5, 50 and 500 μg/mL), which confirms that these polymers are not behaving in similar ways when they are free in solution *vs*. assembled onto nanoparticles. The use of PLA control was not possible due to its limited water solubility.

Although the initial conclusion is that PCB-SCKs can be more immunotoxic than PEG-based nanoparticles, the data were surprising in that even PEG-SCKs can have potential immunotoxicity. Two studies performed by Kiwada and coworkers have confirmed the development of PEG-specific antibodies upon administration of PEG-coated liposomes *in vivo* [28, 29]. Recently, it was recommended to re-evaluate the immunogenicity of approved PEGylated therapeutics in humans, due to evidence that antibodies can be formed against PEG, thus limiting therapeutic efficacy and possibly resulting in severe adverse reactions [30]. Given the fact that PEG is not as inert as has been believed traditionally, the Hawker laboratory has recently developed an exciting new degradable PEG system, aiming to improve the safety profiles of PEG-based polymers and nanomaterials [31]. MCP-1 was the only cytokine that was significantly induced upon treatment with the PEG_{5k}-SCKs. We have evidence from another study that some cytokines, and in particular MCP-1, were significantly induced upon PEGylation of nanoparticles [32]. However, it is worth mentioning that induction of immunotoxicity depends on the overall nanoparticle composition and it is challenging to attribute a particular toxicity to specific components, due to the unrealistic use of homopolymers as controls, which as noted above, cannot emulate the behaviors of the same materials when assembled within a nanoscopic framework.

Although beyond the scope of this study, the immunotoxicity of the uncoated nanoparticles, functionalized or not with DOTA and tyramine, was investigated (Figure 3). The uncoated nanoparticles resulted in high release of most of the measured cytokines. Functionalization with DOTA and tyramine was also observed to enhance the release of the tested cytokines,

as compared to the unfunctionalized SCKs. Although it is difficult to provide direct comparison with the anionic uncoated SCKs, due to differences in size, zeta-potential and composition, it is clear that steric stabilization of nanoparticles is critical in minimizing the toxicity of nanoparticles, even if these polymeric coatings are inducing immunotoxicity *per se*. It is also possible that the difference in immunotoxicity between the PEG- and PCB-nanoparticles is partially due to the better shielding efficiency provided by PEG *vs.* PCB polymers to the PAA-*b*-PLA SCKs.

Anti-biofouling competencies of PEG and PCB as homopolymers or shell-forming polymers on the surface of SCKs

Factors that could influence the immunotoxicity of PEG- and PCB-SCKs could be a difference in cytotoxicity, possible contamination with endotoxins or interference with the multiplexing assay that is utilized to quantify the levels of cytokines. All concentrations of nanomaterials and surfactant tested for their immunotoxicities were not cytotoxic. The levels of endotoxins in the various nanoparticle-formulations were measured using Limulus Amebocyte Lysate assay (Thermo Fisher Scientific Inc., Rockford, IL), and no detectable amounts of endotoxins were identified (data not shown). Further experiments were performed to validate the assay and to test the propensity of nanoparticles to adsorb cytokines. Such experiments would validate the assay, assess the anti-biofouling characteristics of the nanoparticles, and provide an important control for the future use of multiplexing techniques for evaluating the immunotoxicity of nanomaterials. The multiplex assay used in this study is a modified ELISA assay that utilizes capture antibodies immobilized on 6.5 μm color-coded beads to bind specific cytokines (each bead has a specific antibody for a particular cytokine). Then, biotinylated-antibodies are added to form a sandwich-like complex by binding to the cytokine-detection antibody complex, followed by addition of a reporter molecule to form the detection products. Recognition of the beads and fluorescence intensity from the reporter molecules are utilized for detection and quantification of cytokines in the samples, respectively.

The possibility of adsorption of cytokines on the surface of SCKs is supported by earlier reports of cytokine adsorption by nanomaterials. Adsorption of cytokines (*e.g.* GM-CSF, IL-6 and TNF-α) on various types of inorganic nanoparticles (*e.g.* carbon black and titanium oxide nanoparticles) has been observed *in vitro* [33–36]. PEG- and PCB-SCKs, PEG and PCB homopolymers were incubated with a fixed amount of 23 different cytokines mixture, and the concentrations of cytokines were measured and compared to a solution treated in the same way but containing no nanoparticles. The decrease in the apparent concentration of cytokines in the solution containing nanoparticles was then attributed to the adsorption of cytokines or detection antibodies on the surface of nanoparticles or electrostatic and hydrophobic interactions with the polymer chains, with possibility that nanoparticles may interfere with some of the multiplex assay components (antibodies, beads, *etc.*). The adsorption of several cytokines on SCKs and polymers was measured using Bioplex 200 system with HTF and Pro II Wash station (Bio-Rad Laboratories, Inc., Hercules, CA). PCB polymer adsorbed 9 cytokines (G-CSF, IL-4, IL-5, IL-6, IL-10, IL-12(p40), IL-13, MIP-1β and RANTES), while PCB-SCKs adsorbed 18 cytokines (G-CSF, GM-CSF, IFN-γ, IL-2, IL-4, IL-5, IL-6, IL-9, IL-10, IL-12 (p40), IL-12 (p70), IL-13, IL-17, MCP-1, MIP-1β, KC, RANTES and Eotaxin) (Figure 4). On the contrary, PEG polymer reduced the apparent concentration of only one cytokine (G-CSF) and the PEG-SCKs adsorbed 4 cytokines (IL-4, IL-10, IL-12(P40) and MIP-1β). Incubation with Cremophor-EL resulted in adsorption of one cytokine (TNF-α). These data highlight two important concepts. First, the polymers behave differently when they are presented as unimers and when they are in aggregated form, where self-association gives them the ability to cooperatively interact and adsorb the surrounding biomolecules. Second, PCB, probably due to surface zwitterionic charge, had

more adsorption capability than the neutral (non-ionic) PEG, for this particular type of nanomaterials. The uncoated nanoparticles resulted in higher adsorption of the measured cytokines (data not shown), which is expected to be due to the anionic nature of these SCKs and the lack of stealth properties.

Correlation between immunotoxicity, pharmacokinetics and biodistribution

The higher adsorption of proteins on PCB polymers and nanoparticles, as compared to those which were PEGylated, together with the higher *in vitro* immunotoxicity, are well correlated with the longer blood circulation time and lower clearance in the immune organs of the PEG_{5k}-SCKs, as compared to PCB_{5k}-SCKs [17]. The PCB_{2k}-SCKs had a similar or slightly better biodistribution profile than the PEG_{2k} analog. Although the initial study was not focusing on the polymer coating of 2 kDa as they demonstrated inferior physicochemical and *in vivo* characteristics, protein adsorption tendencies and immunotoxicities of PEG_{2k}- and PCB_{2k}-SCKs were investigated to study their relationship to *in vivo* pharmacokinetics of these nanoparticles (Figures 5 and 6). The PCB_{2k}-SCKs adsorbed most of the tested cytokines, as compared to PEG_{2k}-SCKs, which seemed to be a property associated with the PCB polymer, either alone or as a coating on these nanoparticles. Although previous reported data demonstrated lower protein adsorption on PCB grafted polymers as compared to PEG [8, 9], a different assay with different sensitivity limits, protein types, and, importantly, nanoparticle compositions have been utilized in the current study. The immunotoxicity of PEG_{2k}-SCKs was higher than PCB_{2k}-analogs, which is well correlated with *in vivo* pharmacokinetics and biodistribution profiles (Figures 5 and 6) [17]. The PEG_{2k}-SCKs significantly enhanced the secretions of most of the measured cytokines as compared to cells treated with PCB_{2k}-SCKs and control untreated cells. Comparing the type of coating for the PEG_{5k}- and PCB_{5k}-SCKs is reasonable due to the similar physicochemical characteristics (size and zeta-potential values, Table 1). However, SCKs coated with the 2 kDa PCB had three times the size of PEG_{2k}-coated nanoparticles (Table 1). It was reported several times in the literature that nanoparticles of smaller size and larger surface area are associated with higher immunotoxicity [34, 37–39]. Hence, the differences in immunotoxicity and *in vivo* pharmacokinetics observed for the nanoparticles coated with the 2 kDa PEG and PCB chains might be attributed to the size differences of the nanoparticles rather than the type of polymeric coating. It is also observed that SCKs coated with the 2 kDa PEG and PCB resulted in massive release of most of the tested cytokines, as compared to PEG_{5k}- and PCB_{5k}-SCKs, which corroborate the better pharmacokinetic profiles of the nanoparticles coated with PEG and PCB of higher molecular weights, and with the better shielding provided by those polymers as indicated by the almost neutral zeta-potential values, as compared to the negatively-charged surface of nanoparticles coated with the shorter PEG and PCB polymeric chains, and the uncoated nanoparticles. It is worth mentioning that polymer conformation on the surface of nanoparticles can also have an impact on the immunotoxicity of the nanoparticles, as previously reported in the literature [40].

In vivo immunotoxicity of PEG- and PCB-based nanoparticles

Finally, *in vivo* immunotoxicity of PEG_{5k}-SCKs and PCB_{5k}-SCKs was tested for further understanding of the *in vivo* behavior of these nanoparticulates and to study their correlations with the *in vivo* pharmacokinetics and biodistribution profiles of the same nanoparticles. Cremophor-EL, PEG_{5k}-SCKs and PCB_{5k}-SCKs were prepared in phosphate-buffered saline (PBS) and injected into male C57 mice *via* tail vein injection at a dose of 4 mg/kg. The mice were sacrificed 3 h post injection and blood samples were drawn and utilized to prepare serum samples that were further analyzed for concentrations of cytokines using a Bioplex 200 system. In agreement with the PEG and PCB *in vitro* immunotoxicity data, the PCB-coated nanoparticles resulted in secretions of higher amounts of cytokines as

compared to the PEG-coated nanoparticles (Figure 7). Cremophor-EL surfactant had an intermediate immunotoxicity between the PEG- and PCB-based nanoparticles. Clearly, it can be seen that the *in vivo* immunotoxicity of the tested formulations can be ranked as PCB_{5k}-SCKs > Cremophor-EL > PEG_{5k}-SCKs. The PCB_{5k}-SCKs significantly induced secretions of IL-6, IL-10, IL-12 (P70), IL-13, IFN-γ, KC, MCP-1, MIP-lα, as compared to the control animals treated with PBS. Cremophor-EL induced the secretion of several cytokines (IL-2, IL-5, IL-6, IL-13, KC and MCP-1) to a higher extent than the control. On the contrary, secretion of cytokines in response to PEG_{5k}-SCKs was significantly different from the control for only one cytokine (KC). There was consistent increase in several of the tested cytokines in the serum of mice treated with the PEGylated nanoparticles, although the difference was statistically significant for only the KC cytokine. Comparing PEG- *vs.* PCB-coated nanoparticles, the PCB-based nanoparticles induced secretions of most of the tested cytokines to a greater extent than the PEG-coated nanoparticles, although significant differences were found only for three cytokines (IL-6 ($p = 0.04$), MIP-lα ($p = 0.01$) and MCP-1 ($p = 0.008$)).

In summary, advances in polymerization chemistries have enabled the engineering of multifunctional polymeric nanoparticles with precise control over the architectures of the individual polymer components and overall nanoparticle composition, yet much remains to be learned in terms of their compositions, structures, and physicochemical properties in relation to their biological responses *in vitro* and *in vivo*, and there remains a large disconnect between structure-property relationships that rely on molecular-scale parameters and allow for accurate correlation with whole body pharmacokinetics and biodistributions. For instance, when standard *in vitro* and *in vivo* assays were conducted on PCB-*vs*. PEG-coated SCKs, it was difficult to correlate typical physicochemical and cytotoxicity data with *in vivo* pharmacokinetics results. When the stability of SCKs was monitored upon incubation with 10% bovine serum albumin at 37 °C, all nanoparticles were solution stable without undergoing significant aggregation, except for the PCB_{5k}-SCKs, which exhibited a 15% increase in size. PCB-coated nanoparticles showed faster hydrolytic degradation than PEG-coated nanoparticles at both pH 7.4 and 5 [17]. *In vivo* pharmacokinetic evaluation indicated that the PEG_{5k}-SCKs had a longer blood circulation time than that of the corresponding PCB_{5k}-SCKs [17]. Meanwhile, we had noted that Huang and coworkers, and others, have been utilizing the secretions of cytokines in response to treatment of cells and animals with nanoparticles as a measure of nanoparticle immunotoxicity [16, 41–43]. As one example, degradable lipid-coated calcium phosphate nanoparticles that were developed for systemic delivery of siRNA [43] resulted in similar *in vivo* gene silencing to previously developed nanoparticles (DNA/protamine-based complexes), but importantly, induced lower levels of IL-6 and IL-12 cytokines in mice (*i.e.* lower immunotoxicity). Therefore, it was hypothesized that cytokines might be useful as biomarkers for SCK nanoparticle immunotoxicity as well as for prediction of *in vivo* pharmacokinetics and biodistribution profiles of SCK nanomaterials, and we undertook immunotoxicity studies to determine the effects of SCKs toward the induction of cytokines measured *in vitro* from cell studies and *in vivo* in serum samples following intravenous injection of nanoparticle solutions in mice. The *in vitro* and *in vivo* immunotoxicity data revealed that differences in pharmacokinetics could be due to the faster opsonization of PCB-based nanoparticles and the resultant higher immunotoxicity, as compared to PEG-SCKs. Although the hydrophilic polymers that are commonly used to form the shell of nanoparticles show low cytotoxicity, available data on their immunotoxicity are scarce. Here, it was found that the immunotoxicities of the polymer components did not correlate with their behaviors when utilized as nanoparticle-coatings. Therefore, the immunotoxicity of entire nanoparticles can aid, partially, in predicting toxicity, *in vivo* pharmacokinetics and biodistribution profiles of nanomaterials.

The difference in the pattern of cytokines release upon addition of the nanoparticles to the macrophage cell line *in vitro* and upon *in vivo* administration into mice is possibly due to the differences in the environments of cell culture media *in vitro* and the existence of various biomolecules *in vivo*, such as red blood cells, immune cells, plasma proteins and immunoglubulins. However, it is always preferable to develop *in vitro* assays that could predict the *in vivo* behavior of nanoparticles, as it is less time consuming and may reduce the extent and number of required animal experiments. The antibiofouling properties of nanomaterials (lower competencies for adsorbing proteins or other biomolecules in the surrounding medium) and the lower secretions of cytokines upon addition of nanoparticles to macrophages *in vitro* provide a partial prediction of lower opsonization and longer blood circulation time *in vivo*.

The current study highlights the possible use of immunotoxicity assays to predict the *in vivo* characteristics of nanomaterials, and urges the need for rigorous investigation of toxicity and immunogenicity of nanoparticles on individual bases and not just assuming the safety of a particular component. It has been found in this study that the use of PEG instead of PCB as a stealth shell on this particular kind of nanomaterial is promising and was associated with lower *in vitro* and *in vivo* immunotoxicity, and prolonged blood retention in the treated mice. We are not claiming that PEG and PCB polymers are immunotoxic but rather calling for laborious studies of the potential immunotoxicity of specific nanoscopic frameworks that utilize these or other polymer components. It is insufficient to conduct studies on the components alone, rather careful study and explanation of the observed toxicity of nanomaterials are required, as it is inaccurate to affirm the absolute biocompatibility of the hydrophilic polymers that are commonly utilized to form the shells or other regions of nanoparticles.

Acknowledgments

We gratefully acknowledge financial support from the National Heart Lung and Blood Institute of the National Institutes of Health as a Program of Excellence in Nanotechnology (HHSN268201000046C), and the National Institute of Diabetes and Digestive and Kidney Diseases of the National Institutes of Health (R01-DK082546). The Welch Foundation is gratefully acknowledged for support through the W. T. Doherty-Welch Chair in Chemistry, Grant No. A-0001.

REFERENCES

1. Elsabahy M, Wooley KL. Cytokines as biomarkers of nanoparticle immunotoxicity. Chem Soc Rev. 2013; 42:5552–5576. [PubMed: 23549679]
2. Elsabahy M, Shrestha R, Clark C, Taylor S, Leonard J, Wooley KL. Multifunctional Hierarchically Assembled Nanostructures as Complex Stage-Wise Dual-Delivery Systems for Coincidental Yet Differential Trafficking of siRNA and Paclitaxel. Nano Lett. 2013; 13:2172–2181. [PubMed: 23574430]
3. Elsabahy M, Wooley KL. Strategies toward Well-Defined Polymer Nanoparticles Inspired by Nature: Chemistry versus Versatility. J Polym Sci Part A: Polym Chem. 2012; 50:1869–1880.
4. Elsabahy M, Wooley KL. Design of polymeric nanoparticles for biomedical delivery applications. Chem Soc Rev. 2012; 41:2545–2561. [PubMed: 22334259]
5. Le Garrec D, Gori S, Luo L, Lessard D, Smith DC, Yessine MA, Ranger M, Leroux JC. Poly(N-vinylpyrrolidone)-block-poly(D,L-lactide) as a new polymeric solubilizer for hydrophobic anticancer drugs: in vitro and in vivo evaluation. J Control Release. 2004; 99:83–101. [PubMed: 15342183]
6. Lin LY, Lee NS, Zhu J, Nystrom AM, Pochan DJ, Dorshow RB, Wooley KL. Tuning core vs. shell dimensions to adjust the performance of nanoscopic containers for the loading and release of doxorubicin. J Control Release. 2011; 152:37–48. [PubMed: 21241750]

7. Ma Q, Remsen EE, Clark CG Jr, Kowalewski T, Wooley KL. Chemically induced supramolecular reorganization of triblock copolymer assemblies: trapping of intermediate states via a shell-crosslinking methodology. Proc Natl Acad Sci U S A. 2002; 99:5058–5063. [PubMed: 11929963]
8. Carr LR, Zhou Y, Krause JE, Xue H, Jiang S. Uniform zwitterionic polymer hydrogels with a nonfouling and functionalizable crosslinker using photopolymerization. Biomaterials. 2011; 32:6893–6899. [PubMed: 21704366]
9. Jiang S, Cao Z. Ultralow-fouling, functionalizable, and hydrolyzable zwitterionic materials and their derivatives for biological applications. Adv Mater. 2010; 22:920–932. [PubMed: 20217815]
10. Keefe AJ, Jiang S. Poly(zwitterionic)protein conjugates offer increased stability without sacrificing binding affinity or bioactivity. Nature Chem. 2012; 4:59–63. [PubMed: 22169873]
11. Dobrovolskaia MA, McNeil SE. Immunological properties of engineered nanomaterials. Nat Nanotechnol. 2007; 2:469–478. [PubMed: 18654343]
12. Zolnik BS, Gonzalez-Fernandez A, Sadrieh N, Dobrovolskaia MA. Nanoparticles and the immune system. Endocrinology. 2010; 151:458–465. [PubMed: 20016026]
13. Hussain S, Vanoirbeek JA, Hoet PH. Interactions of nanomaterials with the immune system. Wiley Interdiscip Rev Nanomed Nanobiotechnol. 2012; 2:169–183. [PubMed: 22144008]
14. Dobrovolskaia MA, Germolec DR, Weaver JL. Evaluation of nanoparticle immunotoxicity. Nat Nanotechnol. 2009; 4:411–414. [PubMed: 19581891]
15. Tan Y, Li S, Pitt BR, Huang L. The inhibitory role of CpG immunostimulatory motifs in cationic lipid vector-mediated transgene expression in vivo. Hum Gene Ther. 1999; 10:2153–2161. [PubMed: 10498247]
16. Shrestha R, Elsabahy M, Florez-Malaver S, Samarajeewa S, Wooley KL. Endosomal escape and siRNA delivery with cationic shell crosslinked knedel-like nanoparticles with tunable buffering capacities. Biomaterials. 2012; 33:8557–8568. [PubMed: 22901966]
17. Li A, Luehmann HP, Sun G, Samarajeewa S, Zou J, Zhang S, Zhang F, Welch MJ, Liu Y, Wooley KL. Synthesis and in vivo pharmacokinetic evaluation of degradable shell cross-linked polymer nanoparticles with poly(carboxybetaine) versus poly(ethylene glycol) surface-grafted coatings. ACS Nano. 2012; 6:8970–8982. [PubMed: 23043240]
18. Shrestha R, Elsabahy M, Luehmann H, Samarajeewa S, Florez-Malaver S, Lee NS, Welch MJ, Liu Y, Wooley KL. Hierarchically Assembled Theranostic Nanostructures for siRNA Delivery and Imaging Applications. J Am Chem Soc. 2012; 134:17362–17365. [PubMed: 23050597]
19. Nystrom AM, Wooley KL. The Importance of Chemistry in Creating Well-Defined Nanoscopic Embedded Therapeutics: Devices Capable of the Dual Functions of Imaging and Therapy. Acc Chem Res. 2011; 44:969–978. [PubMed: 21675721]
20. Klyachko NL, Manickam DS, Brynskikh AM, Uglanova SV, Li S, Higginbotham SM, Bronich TK, Batrakova EV, Kabanov AV. Cross-linked antioxidant nanozymes for improved delivery to CNS. Nanomedicine. 2012; 8:119–129. [PubMed: 21703990]
21. Kakizawa Y, Harada A, Kataoka K. Glutathione-sensitive stabilization of block copolymer micelles composed of antisense DNA and thiolated poly(ethylene glycol)-block-poly(L-lysine): a potential carrier for systemic delivery of antisense DNA. Biomacromolecules. 2001; 2:491–497. [PubMed: 11749211]
22. Miyata K, Kakizawa Y, Nishiyama N, Yamasaki Y, Watanabe T, Kohara M, Kataoka K. Freeze-dried formulations for in vivo gene delivery of PEGylated polyplex micelles with disulfide crosslinked cores to the liver. J Control Release. 2005; 109:15–23. [PubMed: 16298011]
23. Navath RS, Menjoge AR, Dai H, Romero R, Kannan S, Kannan RM. Injectable PAMAM dendrimer-PEG hydrogels for the treatment of genital infections: formulation and in vitro and in vivo evaluation. Mol Pharm. 2011; 8:1209–1223. [PubMed: 21615144]
24. Moughton AO, O'Reilly RK. Noncovalently connected micelles, nanoparticles, and metal-functionalized nanocages using supramolecular self-assembly. J Am Chem Soc. 2008; 130:8714–8725. [PubMed: 18549205]
25. Fuhrmann K, Schulz JD, Gauthier MA, Leroux JC. PEG Nanocages as Non-sheddable Stabilizers for Drug Nanocrystals. ACS Nano. 2012; 6:1667–1676. [PubMed: 22296103]
26. Zhang S, Zou J, Zhang F, Elsabahy M, Felder SE, Zhu J, Pochan DJ, Wooley KL. Rapid and Versatile Construction of Diverse and Functional Nanostructures Derived from a

Polyphosphoester-Based Biomimetic Block Copolymer System. J Am Chem Soc. 2012; 134:18467–18474. [PubMed: 23092249]

27. ten Tije AJ, Verweij J, Loos WJ, Sparreboom A. Pharmacological effects of formulation vehicles : implications for cancer chemotherapy. Clin Pharmacokinet. 2003; 42:665–685. [PubMed: 12844327]
28. Ishida T, Wang X, Shimizu T, Nawata K, Kiwada H. PEGylated liposomes elicit an anti-PEG IgM response in a T cell-independent manner. J Control Release. 2007; 122:349–355. [PubMed: 17610982]
29. Wang X, Ishida T, Kiwada H. Anti-PEG IgM elicited by injection of liposomes is involved in the enhanced blood clearance of a subsequent dose of PEGylated liposomes. J Control Release. 2007; 119:236–244. [PubMed: 17399838]
30. Garay RP, El-Gewely R, Armstrong JK, Garratty G, Richette P. Antibodies against polyethylene glycol in healthy subjects and in patients treated with PEG-conjugated agents. Expert Opin Drug Deliv. 2012; 9:1319–1323. [PubMed: 22931049]
31. Lundberg P, Lee BF, van den Berg SA, Pressly ED, Lee A, Hawker CJ, Lynd NA. Poly[(ethylene oxide)-co-(methylene ethylene oxide)]: A hydrolytically-degradable poly(ethylene oxide) platform. ACS Macro Lett. 2012; 1:1240–1243. [PubMed: 23205320]
32. Elsabahy M, Samarajeewa S, Raymond JE, Clark C, Wooley KL. Shell-crosslinked knedellike nanoparticles induce lower immunotoxicity than their non-crosslinked analogs. J Mater Chem B. 2013
33. Val S, Hussain S, Boland S, Hamel R, Baeza-Squiban A, Marano F. Carbon black and titanium dioxide nanoparticles induce pro-inflammatory responses in bronchial epithelial cells: need for multiparametric evaluation due to adsorption artifacts. Inhal Toxicol. 2009; 21:115–122. [PubMed: 19558243]
34. Hussain S, Boland S, Baeza-Squiban A, Hamel R, Thomassen LC, Martens JA, Billon-Galland MA, Fleury-Feith J, Moisan F, Pairon JC, Marano F. Oxidative stress and proinflammatory effects of carbon black and titanium dioxide nanoparticles: role of particle surface area and internalized amount. Toxicology. 2009; 260:142–149. [PubMed: 19464580]
35. Kocbach A, Totlandsdal AI, Lag M, Refsnes M, Schwarze PE. Differential binding of cytokines to environmentally relevant particles: a possible source for misinterpretation of in vitro results? Toxicol Lett. 2008; 176:131–137. [PubMed: 18079072]
36. Veranth JM, Kaser EG, Veranth MM, Koch M, Yost GS. Cytokine responses of human lung cells (BEAS-2B) treated with micron-sized and nanoparticles of metal oxides compared to soil dusts. Part Fibre Toxicol. 2007; 4:2. [PubMed: 17326846]
37. Monteiller C, Tran L, MacNee W, Faux S, Jones A, Miller B, Donaldson K. The pro-inflammatory effects of low-toxicity low-solubility particles, nanoparticles and fine particles, on epithelial cells in vitro: the role of surface area. Occup Environ Med. 2007; 64:609–615. [PubMed: 17409182]
38. Singh S, Shi T, Duffin R, Albrecht C, van Berlo D, Hohr D, Fubini B, Martra G, Fenoglio I, Borm PJ, Schins RP. Endocytosis, oxidative stress and IL-8 expression in human lung epithelial cells upon treatment with fine and ultrafine TiO2: role of the specific surface area and of surface methylation of the particles. Toxicol Appl Pharmacol. 2007; 222:141–151. [PubMed: 17599375]
39. Wittmaack K. In search of the most relevant parameter for quantifying lung inflammatory response to nanoparticle exposure: particle number, surface area, or what? Environ Health Perspect. 2007; 115:187–194. [PubMed: 17384763]
40. Hamad I, Al-Hanbali O, Hunter AC, Rutt KJ, Andresen TL, Moghimi SM. Distinct polymer architecture mediates switching of complement activation pathways at the nanosphere-serum interface: implications for stealth nanoparticle engineering. ACS Nano. 2010; 4:6629–6638. [PubMed: 21028845]
41. Chono S, Li SD, Conwell CC, Huang L. An efficient and low immunostimulatory nanoparticle formulation for systemic siRNA delivery to the tumor. J Control Release. 2008; 131:64–69. [PubMed: 18674578]
42. Li SD, Chono S, Huang L. Efficient oncogene silencing and metastasis inhibition via systemic delivery of siRNA. Mol Ther. 2008; 16:942–946. [PubMed: 18388916]

43. Li J, Chen YC, Tseng YC, Mozumdar S, Huang L. Biodegradable calcium phosphate nanoparticle with lipid coating for systemic siRNA delivery. J Control Release. 2010; 142:416–421. [PubMed: 19919845]

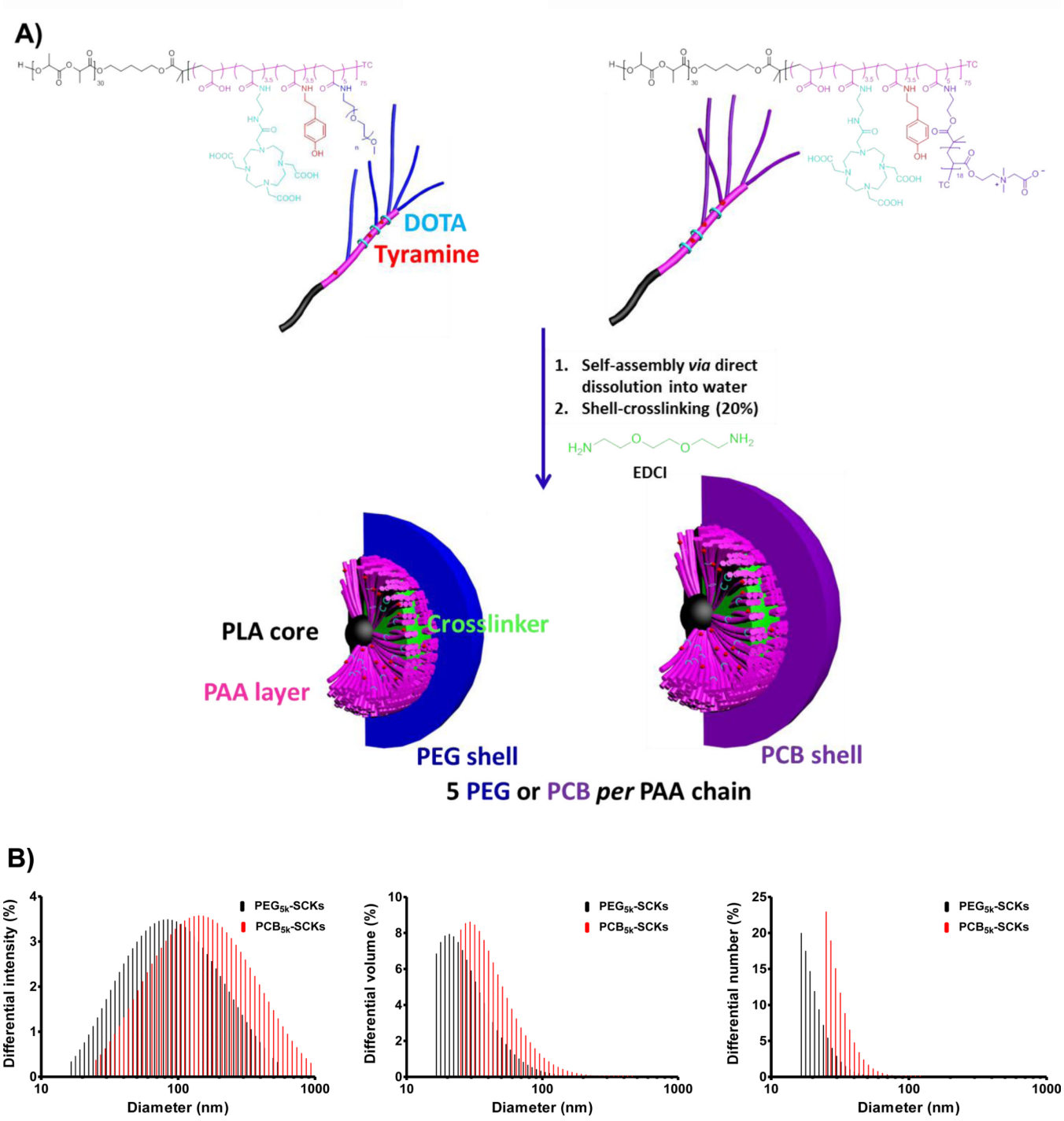

Figure 1.

(A) Chemical structures of DOTA- and tyramine-functionalized PEG- and PCB-*g*-PAA-*b*-PLA copolymers, their self-assembly in water and crosslinking to form SCKs, with PLA degradable cores, PAA crosslinked shells, DOTA and tyramine available functionalities, and a hydrophilic shell of either PEG or PCB. (B) Characterizations of PEG_{5k}- and PCB_{5k}-based SCKs in terms of intensity-, volume- and number-averaged hydrodynamic diameter histograms in Tris buffer (10 mM, pH 7.4).

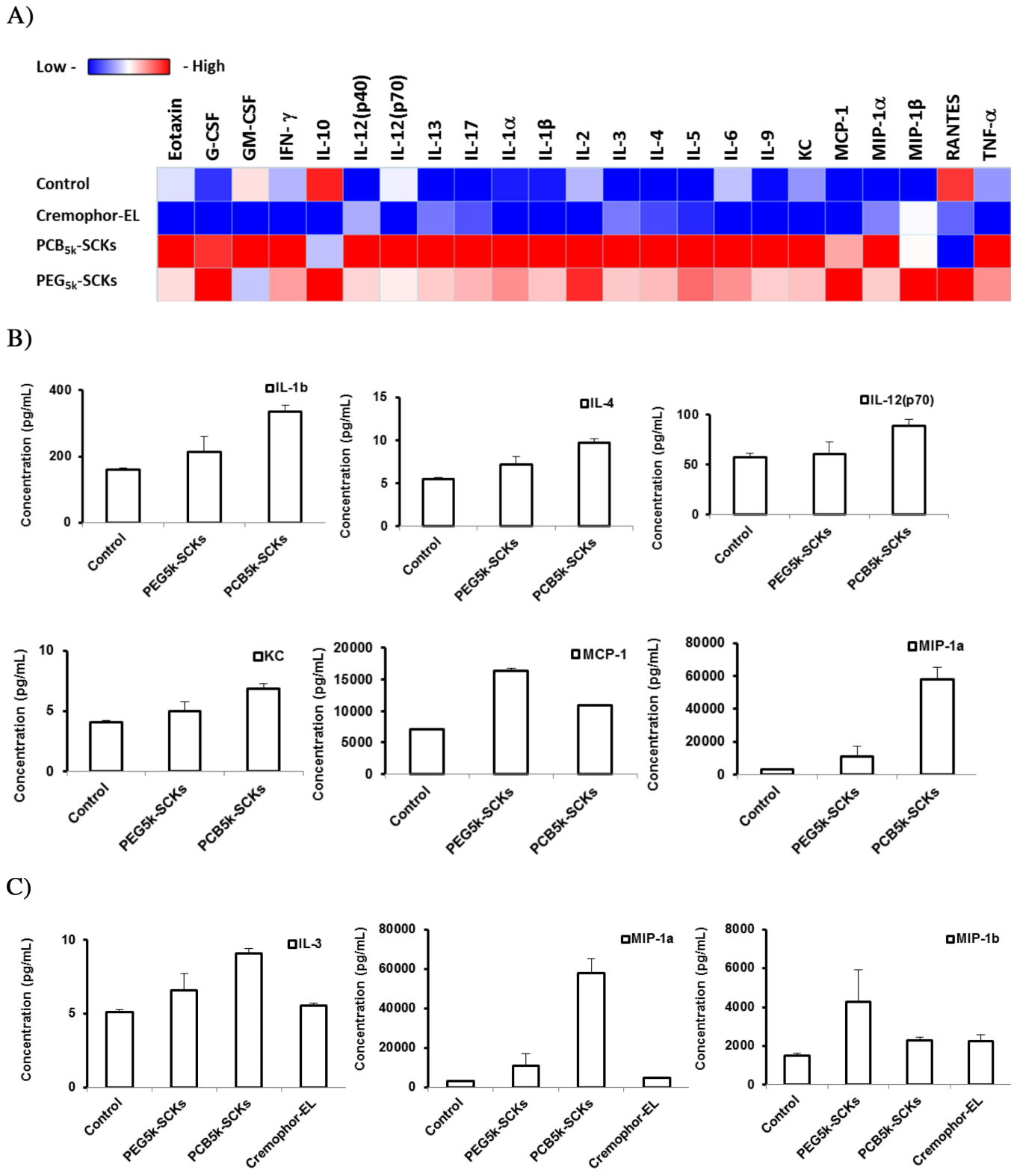

Figure 2.

(A) Heat map of the relative expression of mouse cytokines, interleukin (IL)-lα, IL-1β, IL-2, IL-3, IL-4, IL-5, IL-6, IL-9, IL-10, IL-12 (P40), IL-12 (P70), IL-13, IL-17, Eotaxin,

granulocyte-colony-stimulating factor (G-CSF), granulocyte macrophage-colony-stimulating factor (GM-CSF), interferon-γ (IFN-γ), keratinocyte-derived chemokine (KC), monocyte chemotactic protein (MCP)-l, macrophage inflammatory protein (MIP)-lα, MIP-1β, regulated upon activation normal T-cell expressed and presumably secreted (RANTES) and tumor necrosis factor-α (TNF-α) following the treatment of RAW 264.7 cells with media (control), PEG- or PCB-based SCKs and Cremophor-EL. (B) The expression of cytokines that were significantly enhanced upon treatment with the two nanoparticle-formulations. (C) The expression of cytokines that were significantly enhanced upon treatment with Cremophor-EL surfactant.

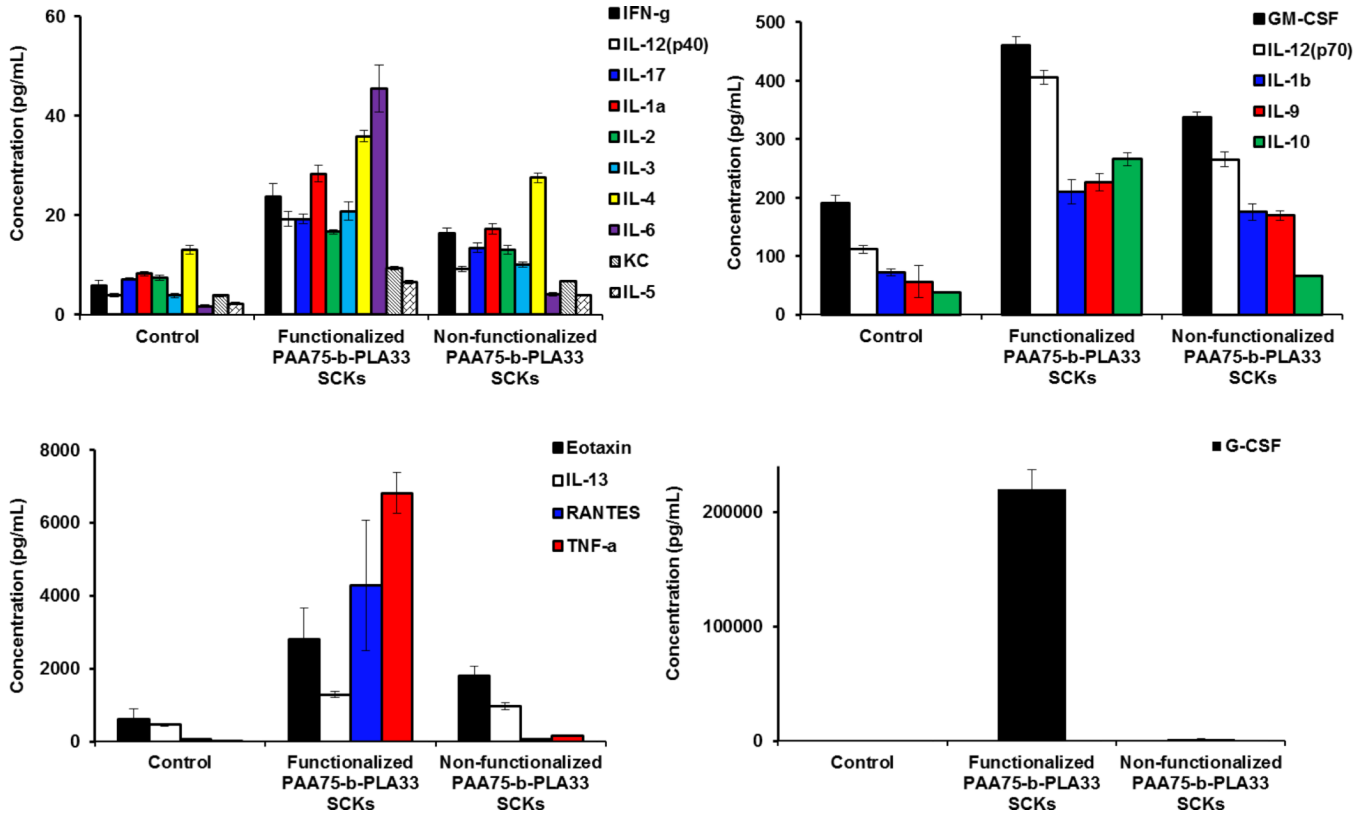

Figure 3.

The relative expression of mouse cytokines, IL-1α, IL-1β, IL-2, IL-3, IL-4, IL-5, IL-6, IL-9, IL-10, IL-12 (P40), IL-12 (P70), IL-13, IL-17, Eotaxin, G-CSF, GM-CSF, IFN-γ, KC, RANTES and TNF-α following the treatment of RAW 264.7 cells with media (control), PAA_{75}-*b*-PLA_{33} SCKs, functionalized or not with DOTA and tyramine.

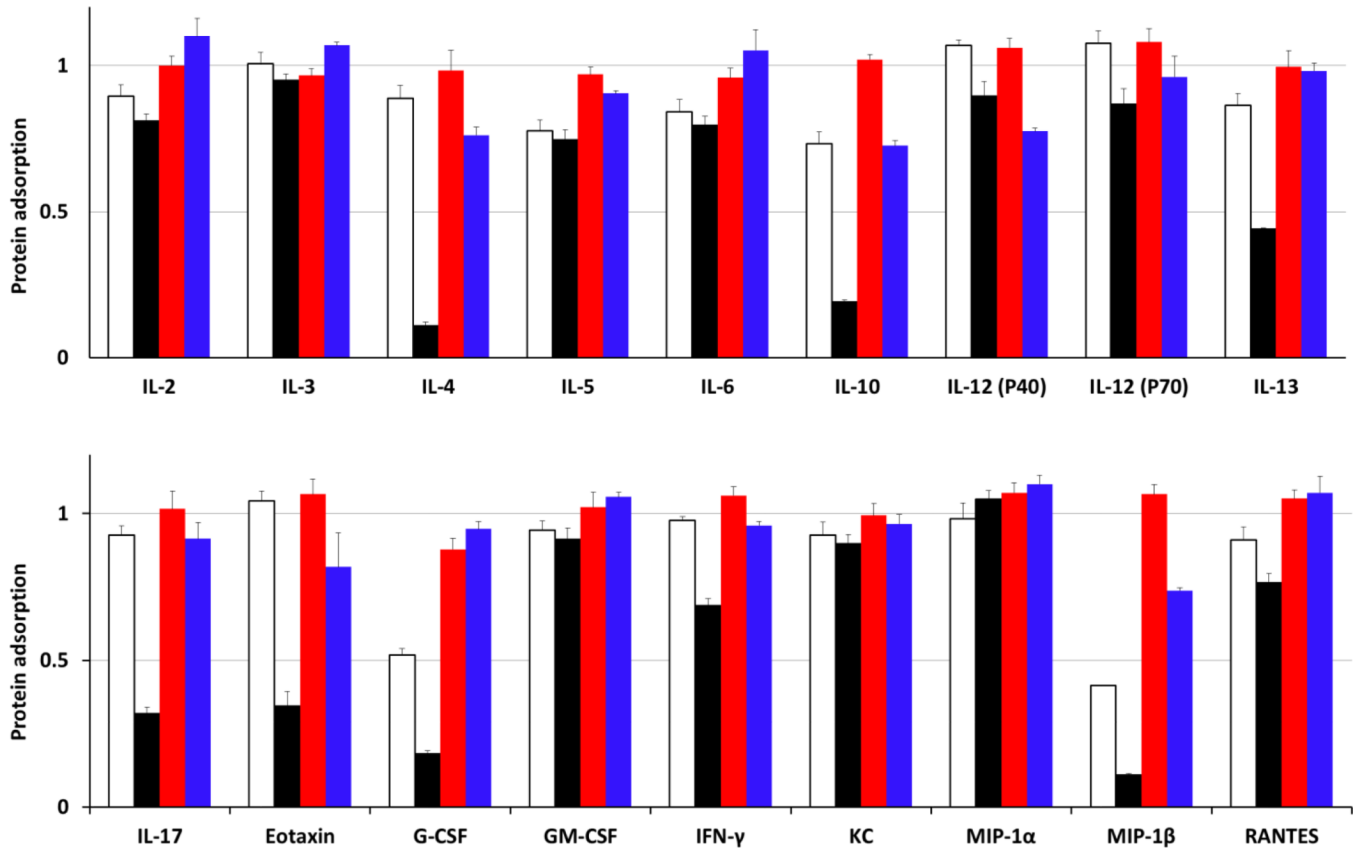

Figure 4.

Adsorption of IL-2, IL-3, IL-4, IL-5, IL-6, IL-10, IL-12 (P40), IL-12 (P70), IL-13, IL-17, Eotaxin, G-CSF, GM-CSF, IFN-γ, KC, MIP-lα, MIP-1β and RANTES cytokines by PCB_{5k} polymer (white bars), PEG_{5k} polymer (red bars), PCB_{5k}-SCKs (black bars) and PEG_{5k}-SCKs (blue bars). The values are presented as the ratio of concentration of the cytokines in the cytokines/nanoparticles mixture (500 μg/mL polymers or nanoparticles) to that in a solution that contains the same amount of the cytokines but without nanoparticles.

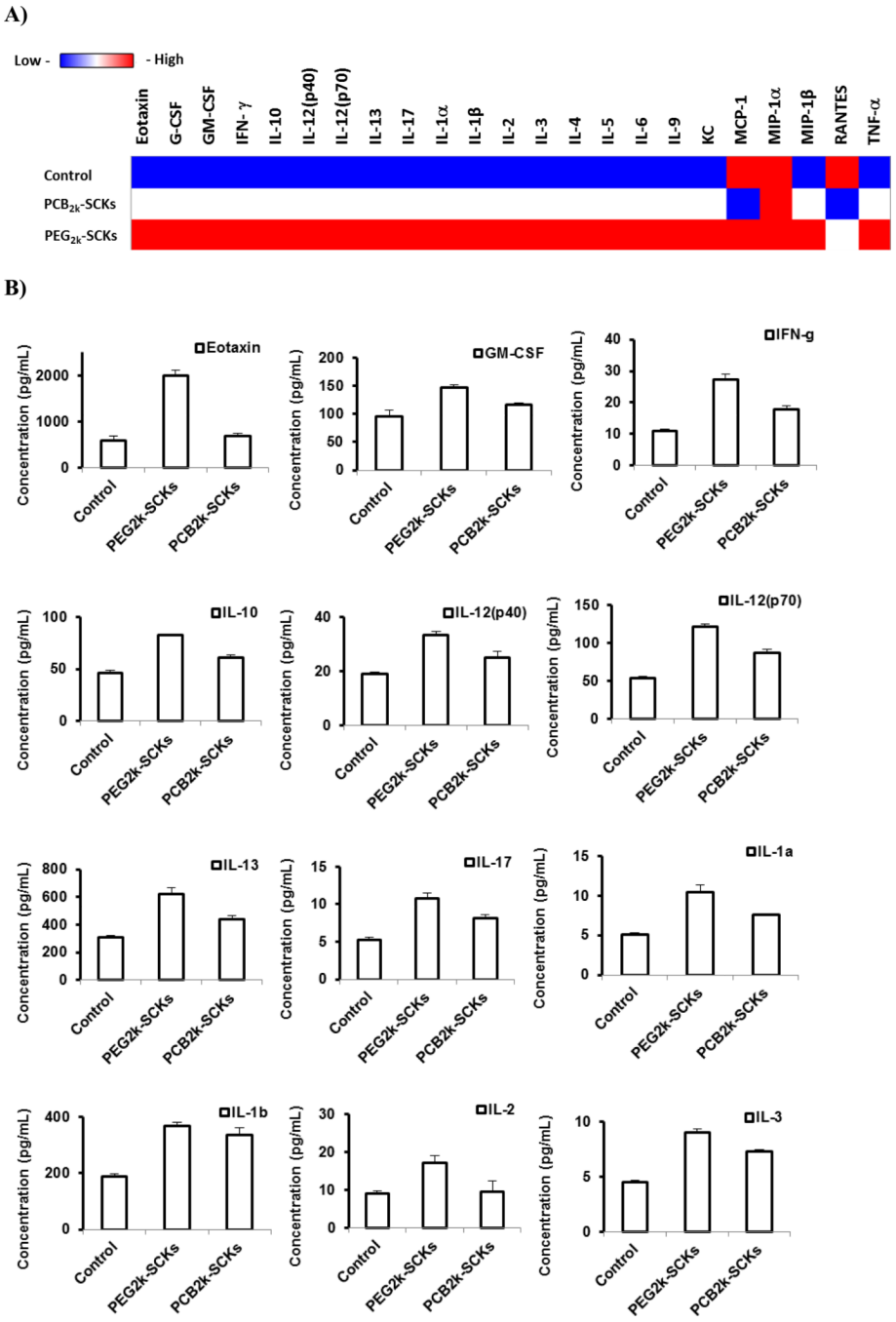

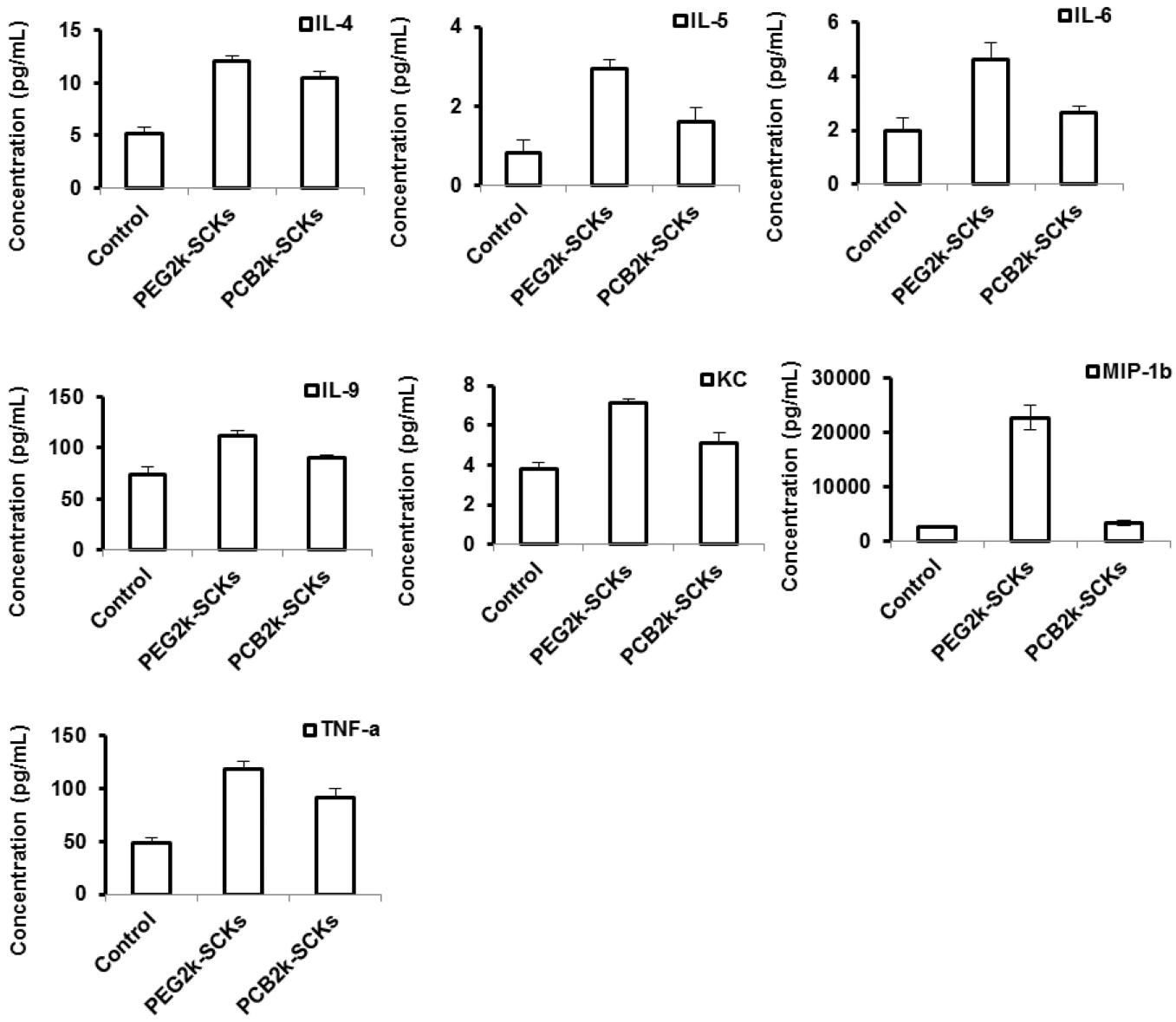

Figure 5.

(A) Heat map of the relative expression of 23-mouse cytokines following the treatment of RAW 264.7 cells with media (control), PEG_{2k}- and PCB_{2k}-based SCKs. (B) The expression of cytokines that were significantly enhanced upon the treatment with the two nanoparticle-formulations.

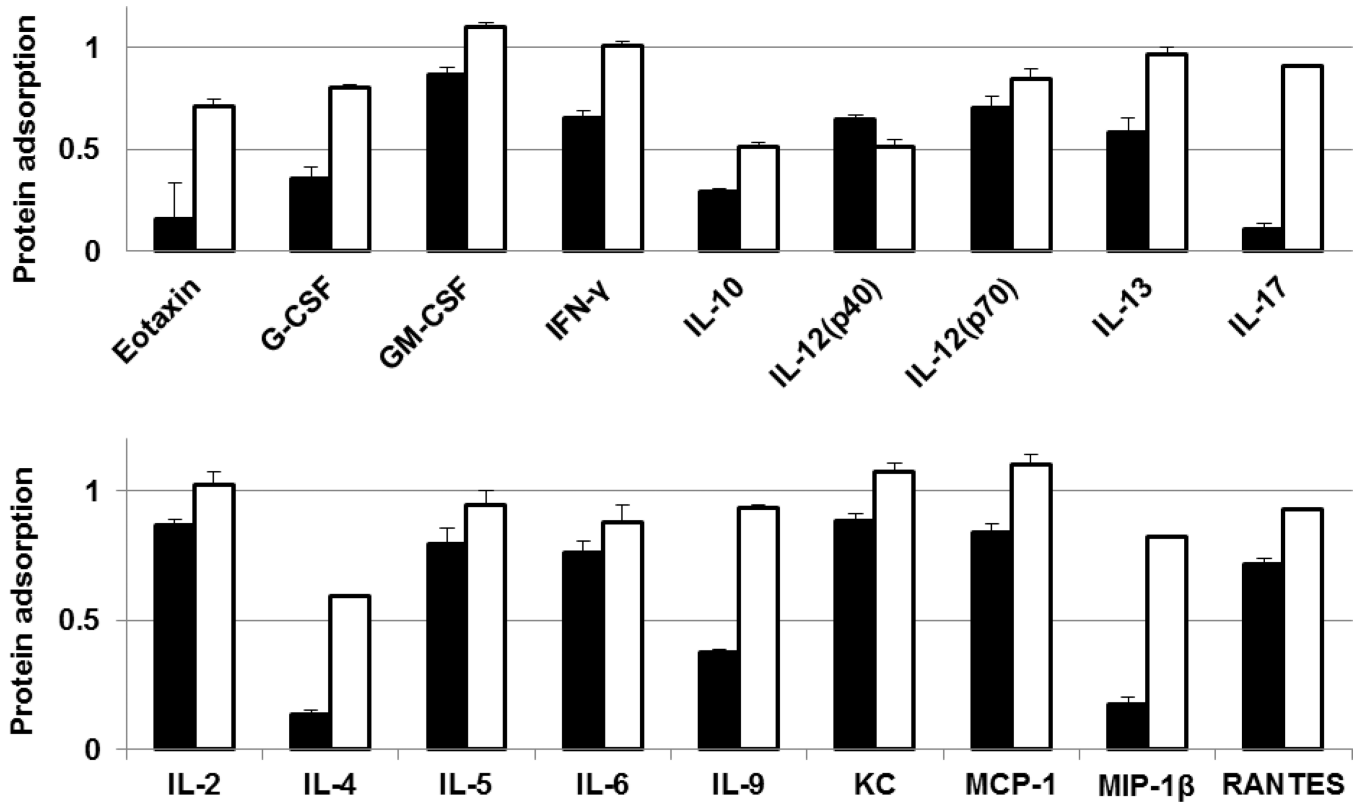

Figure 6.

Adsorption of IL-2, IL-4, IL-5, IL-6, IL-9, IL-10, IL-12 (P40), IL-12 (P70), IL-13, IL-17, Eotaxin, G-CSF, GM-CSF, IFN-γ, KC, MCP-1, MIP-1β and RANTES cytokines by PCB_{2k}-SCKs (black bars) and PEG_{2k}-SCKs (white bars). The values are presented as the ratio of cytokines in the cytokines/nanoparticles mixture (500 μg/mL polymers or nanoparticles) to the solution that contain the same amount of the cytokines but without the nanoparticles.

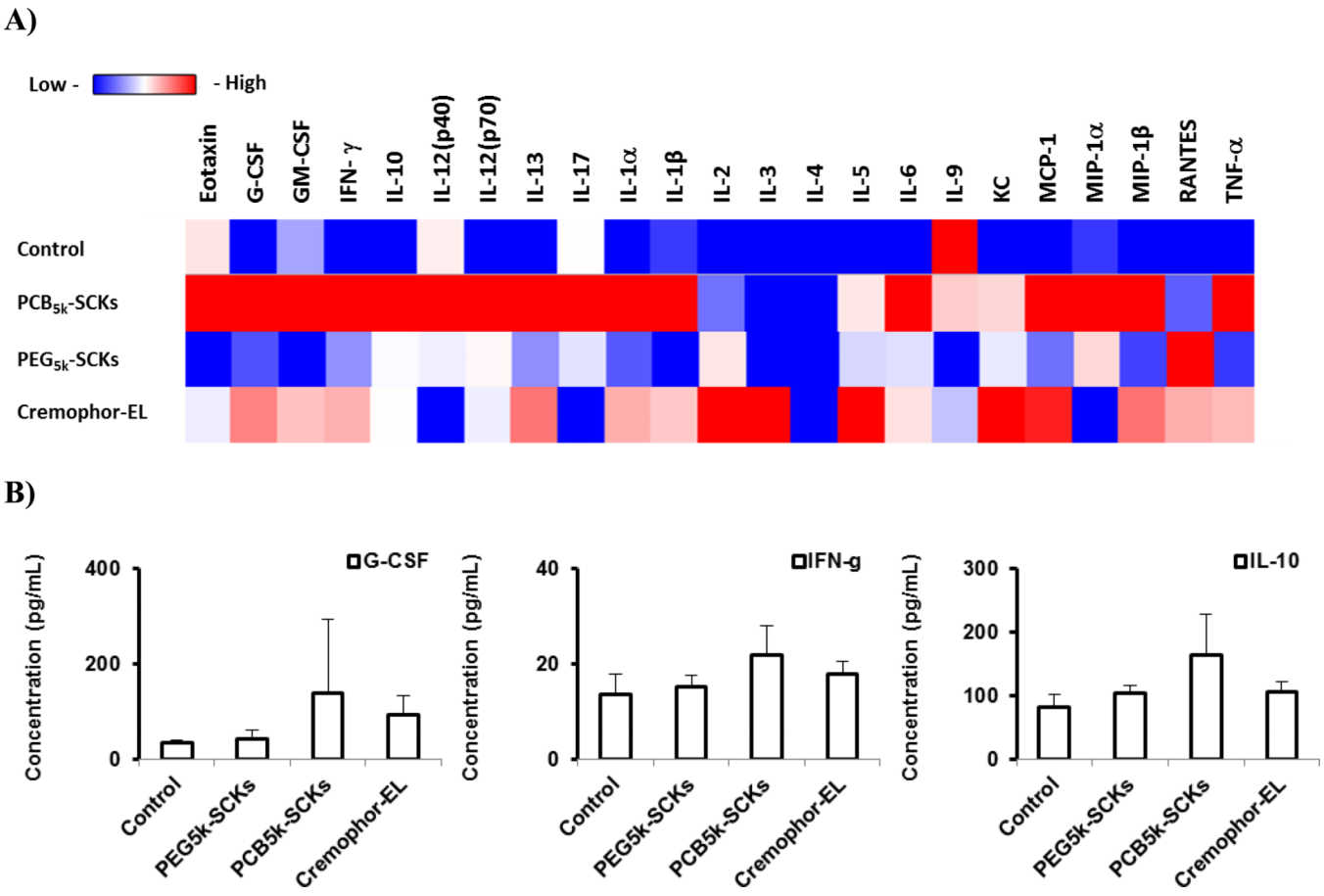

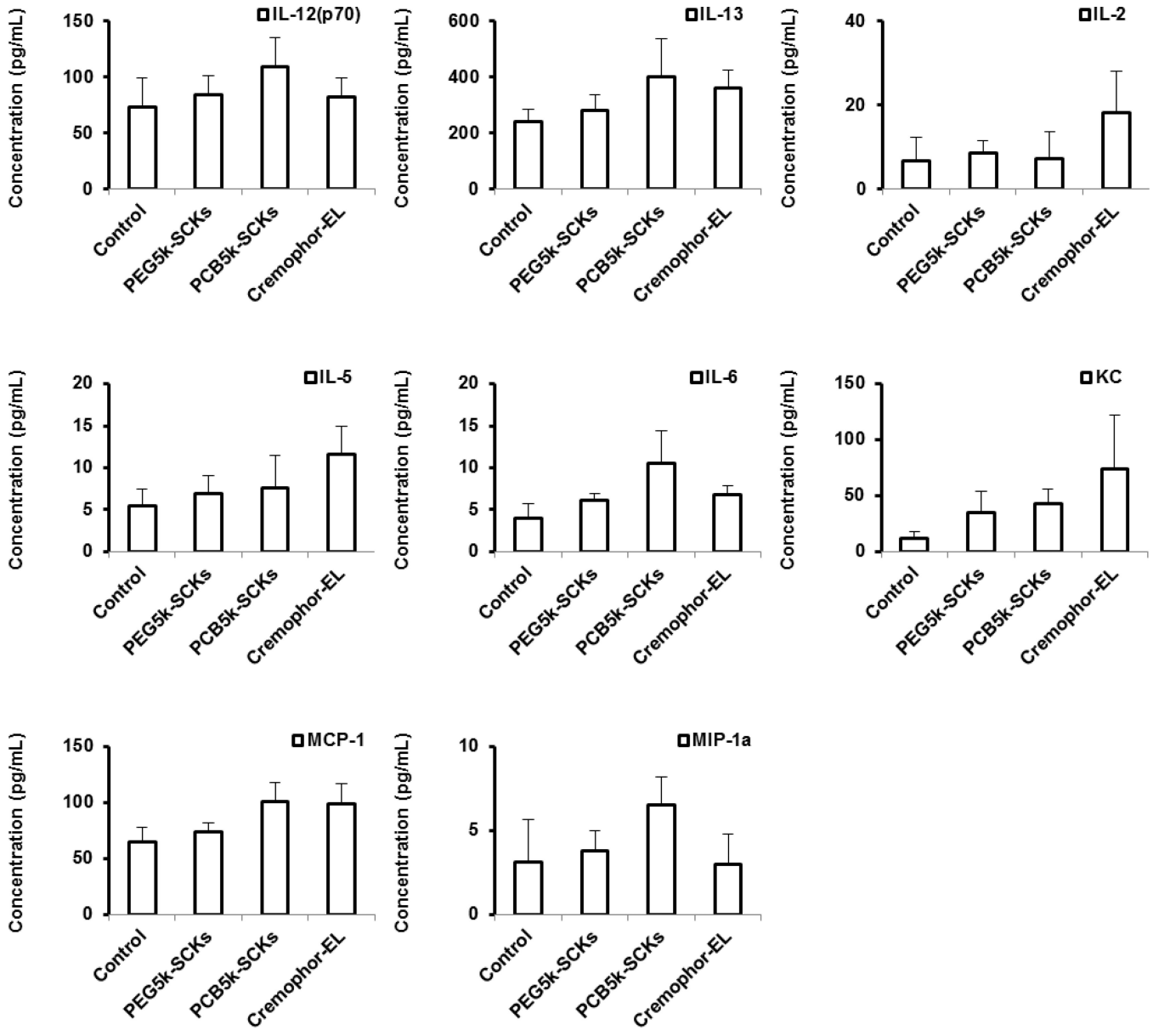

Figure 7.

(A) Heat map of the relative expression of 23-mouse cytokines in serum of mice treated with PBS (control), PEG_{5k}- or PCB_{5k}-based SCKs and Cremophor-EL at 4 mg/kg. **(B)** The expression of cytokines that were significantly enhanced upon treatment with the two nanoparticle-formulations and Cremophor-EL surfactant.

Table 1

Characterizations of PEG- and PCB-based SCKs, PAA_{75}-*b*-PLA_{33} SCKs, functionalized or not with DOTA and tyramine, in terms of intensity-, volume- and number-averaged hydrodynamic diameters, polydispersity indices (PDI) and zeta-potentials in Tris buffer (10 mM, pH 7.4).

SCKs	I-averaged diameter (nm)	V-averaged diameter (nm)	N-averaged diameter (nm)	PDI	Zeta-potential (mV)
PEG_{5k}-SCKs	122 ± 3	26 ± 4	18 ± 3	0.3 ± 0.03	−0.3 ± 0.1
PCB_{5k}-SCKs	200 ± 3	48 ± 4	32 ± 1	0.3 ± 0.01	−4.5 ± 2.2
PEG_{2k}-SCKs	290 ± 4	46 ± 2	31 ± 1	0.3 ± 0.05	−27 ± 5.4
PCB_{2k}-SCKs	225 ± 3	124 ± 0.4	90 ± 0.3	0.22 ± 0.005	−36 ± 1.8
Unfunctionalized PAA_{75}-*b*-PLA_{33}	473 ± 14	91 ± 3	61 ± 3	0.21 ± 0.003	−34 ± 1.7
DOTA- and tyramine-functionalized PAA_{75}-*b*-PLA_{33}	358 ± 2	80 ± 3	53 ± 2	0.28 ± 0.01	−37± 1.5